Sde Proteins Coordinate Ubiquitin Utilization and Phosphoribosylation to Promote Establishment and Maintenance of the *Legionella* Replication Vacuole

Running Title: Sde-mediated deubiquitination and ubiquitin phosphoribosylation.

Key terms: *Legionella*, macrophages, autophagy, ubiquitination, deubiquitination, intracellular replication

Figs: 1-6

Supplemental figs: 1-2

Supplemental Table 1-2

Kristin M. Kotewicz[1,2#], Mengyun Zhang[1,3#], Seongok Kim[1#], Albert Tai[4], and Ralph R. Isberg[1,4]

[#] These authors contributed equally to this work

[1] Department of Molecular Biology and Microbiology, Tufts University School of Medicine, 150 Harrison Ave., Boston, MA 02111, USA
[2] Current address: Gastrointestinal Unit and Center for the Study of Inflammatory Bowel Disease, Massachusetts General Hospital, Harvard Medical School, Boston, MA 02114
[3] Current address: Global Health Drug Discovery Institute, Haidian, Beijing, China
[4]Department of Developmental, Molecular and Chemical Biology, Tufts University School of Medicine, 150 Harrison Ave., Boston, MA 02111, USA

Abstract

The *Legionella pneumophila* Sde family of translocated proteins promote host tubular endoplasmic reticulum (ER) rearrangements that are tightly linked to phosphoribosyl-ubiquitin (pR-Ub) modification of Reticulon 4 (Rtn4). Sde proteins have two additional activities of unclear relevance to the infection process: K63 linkage-specific deubiquitination and phosphoribosyl modification of polyubiquitin (pR-Ub). We show here that the deubiquitination activity (DUB) stimulates ER rearrangements while pR-Ub protects the replication vacuole from cytosolic surveillance by autophagy. Loss of DUB activity was tightly linked to lowered pR-Ub modification of Rtn4, consistent with the DUB activity fueling the production of pR-Ub-Rtn4. In parallel, phosphoribosyl modification of polyUb, in a region of the protein known as the isoleucine patch, caused an absolute block in binding by the autophagy adapter p62. An inability of Sde mutants to modify polyUb resulted in immediate p62 association, a critical precursor to autophagic attack. The ability of Sde WT to block p62 association decayed quickly after bacterial infection, as predicted by the presence of previously characterized *L. pneumophila* effectors that inactivate Sde and remove polyUb. In sum, these results show that the accessory Sde activities act to stimulate ER rearrangements and protect from host innate immune sensing in a temporal fashion.

Introduction

Legionella pneumophila is a facultative intracellular bacterium that is the causative agent of Legionnaire's disease, a pneumonia of high lethality that primarily occurs in the immunocompromised and individuals with depressed lung function[1, 2]. Disease is usually associated with aspiration of droplets from contaminated water sources harboring amoebae that act as the environmental intracellular reservoir to support growth of the bacterium[3]. Once deposited within the lungs, productive infection involves growth of *L. pneumophila* within alveolar macrophages followed by attempted neutrophil clearing, which accumulates during productive pneumonic disease[4]. The ability of the bacterium to grow within macrophages is tightly linked to an environmental lifestyle that involves growth within amoebae, as establishing a niche within amoebal species provides the selective pressure for acquisition of genes that promote intracellular growth[5, 6]. Therefore, human disease promoted by the bacterium is a consequence of targeting host cell functions that are largely conserved from amoebae to man.

Intracellular growth of *L. pneumophila* requires construction of the *Legionella*-containing vacuole (LCV), which is derived from host membranes and is tightly associated with host endoplasmic reticulum and the early secretory apparatus[7, 8]. The LCV avoids interaction with the endocytic pathway including the highly antimicrobial lysosome[9]. Biogenesis of the bacterial compartment requires the function of the Icm/Dot type IV secretion system that acts as a syringe to deposit translocated bacterial effector proteins into the surrounding membrane as well as into the cytosol[10, 11]. Every *Legionella* species member encodes at least 300 of these effectors, which are remarkably poorly conserved, with only seven proteins found in all species[12, 13]. The biochemical activities of a large number of these proteins have been identified, many of which perform posttranslational modifications (PTMs) on host proteins, conferring activation, inhibition, altered regulation or acquisition of new functions on the target proteins[14]. The most notable consequences of these activities are to maintain the integrity of the LCV[15], promote association with proteins involved in endoplasmic reticulum dynamics[16], inactivate host

76 components that drive association with the endocytic compartment [17], and inhibit protein
77 synthesis[18].
78 One set of Icm/Dot system translocated proteins that drives a unique morphological
79 transformation of the LCV is the Sde family (SidE, SdeA, SdeB and SdeC)[19, 20, 21, 22]. The
80 importance of this family is emphasized by the discovery that at least five other *L. pneumophila*
81 translocated substrates regulate the dynamics of this family[23, 24, 25, 26, 27, 28]. As is true of many
82 Icm/Dot substrates, each member is a composite of three enzymatic activities located on separate
83 domains (Fig. 1A)[29, 30, 31]. A mono-ADPribosyltransferase (mART) domain drives NAD-
84 dependent ADPribosylation of diverse ubiquitin species at Arginine 42 (ADPr-Ub)[20, 22]. In turn, a
85 phosphodiesterase-like domain (PDE) can use ADPr-Ub to either promote phosphoribosyl
86 linkage of Ub (pR-Ub) to substrates, or hydrolysis to generate free phosphoribosylated-Ub[21, 22].
87 The DUB domain is an accessory activity that preferentially deubiquitinates Lys63-linked
88 polyubiquitin chains[32]. A number of potential mammalian substrates have been shown to be pR-
89 Ub modified by Sde members on serine residues that are located in relatively unstructured
90 regions of proteins[29, 30]. Work with model substrates indicates that tyrosine residues may also be
91 targeted[33]. Although the number of Sde substrates is likely to be quite large given the structural
92 preference for pR-Ub modification, modifications of endoplasmic reticulum protein Rtn4[22] and
93 Golgi-associated GRASP family members appear most closely tied to events involved in LCV
94 biogenesis[27, 34]. In the absence of DUB activity, there is accumulation of polyUb about the
95 replication vacuole, with unknown consequences on replication vacuole formation or
96 intracellular growth[32].
97 Immediately after *L. pneumophila* is internalized by macrophages, pR-Ub modification of
98 Rtn4 drives replication vacuole association with endoplasmic reticulum tubules. This modification
99 results in highly detergent-resistant structures that appear to wall off the LCV from the host cell
100 cytosol[22], in a process that contributes to the protection of the LCV from attack by early endosomal
101 components that degrade the vacuole[35]. Simultaneously, there is accumulation of
102 polyubiquitinated targets about the LCV[36, 37, 38, 39, 40], which appear to be targets of the Sde DUB

103 domain[32, 41]. Phosphoribosyl modification of polyUb by Sde proteins stabilizes these structures, by
104 blocking wholesale reversal of polyubiquitination by both bacterial and host DUBs[42].
105 Accumulation of polyUb potentially provides a target for the host cell autophagy pathway that
106 could drive degradation of the LCV[43, 44, 45]. *L. pneumophila* appears to have several systems for
107 blocking autophagic recognition of the LCV, including degradation of central components of the
108 autophagy machinery by the Icm/Dot effector RavZ[46], degradation of syntaxin 17 by effector
109 Lpg1137[47], as well as the described phosphoribosylation[48].
110 In this study, we report the role of the DUB and phosphoribosylation accessory activities
111 of Sde family members. We show that the DUB domain surprisingly increases the efficiency of
112 Rtn4 mobilization about the LCV, while ADPribosylation or phosphoribosylation of Ub
113 interferes with autophagy by causing an absolute physical block on binding of polyUb to an
114 autophagy adaptor, primarily by phosphoribosylation of target Ub chains about the LCV.
115 Similar results have been obtained in the simultaneously submitted manuscript by Wan, *et al.*[49]
116
117
118
119
120
121
122
123

Results

The Sde DUB activity is required for efficient Rtn4 rearrangements in response to *L. pneumophila*.

To determine if there is a link between the Sde family K63 deubiquitinase (DUB) domain (Fig. 1A) and biogenesis of the *Legionella*-containing vacuole (LCV), the kinetics of polyubiquitin (polyUb) association and Rtn4 rearrangements about the LCVs were analyzed. A previous study had shown that the absence of the DUB domain resulted in a 2-fold increase in polyUb about the LCV[32]. Bone marrow-derived macrophages (BMDMs) were challenged with *L. pneumophila* derivatives lacking either the complete complement of *sde* family members (*sidE*, *sdeABC*) or missing *sdeABC* (Δ*sdeC-A*), which removes all proteins known to control Rtn4 dynamics[19]. After 5 min centrifugation onto BMDMs, followed by fixation and probing with a polyUb-specific antibody (FK1), there was no evidence of polyUb about the LCV of WT strains (Fig. 1B; 0 minutes post infection (MPI)). In contrast, challenge with *L. pneumophila* missing all *sde* family members (Δ*sde*) resulted in over 30% of the LCVs displaying polyUb association. By 10 MPI, ~15% of the vacuoles containing WT strain positively stained with polyUb, approximately 4X lower than the Δ*sde* strain at this timepoint, consistent with previous observations (Fig. 1B; [32]). At 0 MPI, Δ*sde* mutants were efficiently complemented by all three members of the Sde family known to have biological activity (SdeA, SdeB and SdeC; Fig. 1B), although complementation of Δ*sdeC-A* mutants retaining SidE was weaker (Fig. 1C). Surprisingly, for all complemented strains, polyUb quickly rose to the levels seen in the absence of Sde family function (Fig. 1B,C; 30 MPI).

The ability to prevent polyUb association with the LCV at the earliest timepoint was dependent on the activity of the DUB domain, as the SdeC-C118S active site mutation was unable to block polyUb association at the earliest timepoint (Fig. 1C; 0 MPI). We conclude that inhibition of the polyUb association with the LCV occurs transiently and is dependent on the Sde deubiquitinase activity. The fact that the inhibition is transient is consistent with the LCV-

151 associated polyUb chains becoming resistant to the action of the DUB domain by 30 minutes
152 post-infection (MPI).
153 The biological significance of having a K63 deubiquitinase activity is unclear, especially
154 because the ART activity of Sde proteins directly blocks deubiquitination, arguing that the DUB
155 may play some role other than reducing LCV polyubiquitination [22, 42]. Alternatively, the DUB
156 activity could modulate the dynamics of Rtn4 rearrangements about the LCV[22]. To test this
157 model, BMDMs were challenged with *L. pneumophila* derivatives having defective DUB
158 activity followed by probing for Rtn4 detergent-resistant structures about the LCV (Figs. 1D,E)
159 [22]. Surprisingly, the inactive DUB mutant (C118S) reduced Rtn4 colocalization with the LCV.
160 In strains expressing either SdeA, SdeB or SdeC as the sole demonstrated drivers of Rtn4
161 rearrangement, the C118S mutation reduced detergent-resistant Rtn4 association with the LCV
162 by approximately 50% (Figs. 1D,E). Plasmid-borne SdeA showed lowered complementation
163 levels (Figs. 1D,E), but SdeA also drove detergent-resistant Rtn4 structures that were not LCV-
164 associated, indicating that SdeA overproduction may result in leakage of the protein from the
165 LCV, as has been documented previously[19].
166 Consistent with data in Fig. 1E, Rtn4 association with the LCV was robust in strains
167 expressing SdeB or SdeC as the sole plasmid-expressed isoforms (Figs. 1I,J) and
168 indistinguishable from the WT strain (Fig. 1F). In contrast, loss of *sdeC-A* prevented Rtn4
169 association with the LCV, as did elimination of the T4SS (Figs. 1G, H). The presence of the
170 C118S mutation resulted in two populations, with a mixture of robust Rtn4-colocalization with
171 LCVs or RTN4 staining below the level of detection (Fig. 1K). Similar results were seen with the
172 DUB D80A catalytic mutant, whereas a control Cys mutant C293S showed high levels of
173 colocalization (Fig. S1). These results are consistent with the DUB domain playing a role in
174 LCV biogenesis at the level of controlling Rtn4 dynamics.
175 To test if the Sde DUB activity plays a direct role in promoting Rtn4 rearrangements, we
176 determined if the catalytic domain contributed to the rate of Sde-dependent phosphoribosyl-
177 ubiquitin (pR-Ub) modification of Rtn4. In a purified system, pR-Ub modification of Rtn4 is

178 rapid and robust with the presence of excess mono-Ub[22, 33]. In contrast, infection provides
179 multiple potential sources of Ub, including K63-linked polyUb, which the DUB activity could
180 target to provide substrate for pR-Ub modification. To test this hypothesis, HEK293T cells
181 transfected with HA-Ub were challenged by *L. pneumophila* harboring either WT or DUB-
182 defective (C118S) derivatives as the only active Sde family members. At 10 or 180 MPI, cells
183 were extracted and subjected to immunoprecipitation with anti-Rtn4, followed by
184 immunoprobing with anti-HA to reveal Rtn4 ubiquitination (Fig. 1L). Detectable mono- and di-
185 modification of the Rtn4B and Rtn4B2 isoforms were observed as early as 10 MPI with
186 continued increase at 180 MPI in response to the WT strain (Fig. 1L, WT). In contrast, challenge
187 with Δ*sde* mutants showed HA-Ub modification that was indistinguishable from mock-infected
188 controls (Fig. 1M; vector vs. Mock). Challenge with Δ*sde* mutants harboring single SdeA or
189 SdeB isoforms each showed rescue of the HA-Ub modification defect, and their rescue was
190 largely eliminated by the presence of the C118S catalytic mutation (Fig. 1M; compare p*sdeA* and
191 *psdeB* to the respective C118S derivatives). Therefore, the absence of Sde DUB activity results
192 in a strong reduction in both detergent-resistant Rtn4 and Ub modification of Rtn4, strongly
193 arguing that Sde-mediated deubiquitination of K63-linked polyUb plays a role in LCV dynamics,
194 possibly providing a pool of mono-Ub substrate for the ART domain.
195
196 **ADPribosylation of ubiquitin by Sde results in hyper-ubiquitination of the LCV.**
197 The data that polyUb association with the LCV occurs robustly immediately after
198 bacterial contact in the absence of the DUB domain argues that the likely role of pR-
199 modification is to stabilize polyUb (Fig. 1). Furthermore, both pR-modification and ADP-
200 ribosylation by Sde block bacterial DUBs as well as a variety of host-encoded K63- and K48-
201 specific DUBs (Fig. 2A)[42], arguing that pR modification of Ub does not play a significant role in
202 blocking polyubiquitination during LCV formation as proposed previously[21].
203 The *L. pneumophila sdeC*$_{H416A}$ (PDE^{-}) mutant results in ADPr modification of Ub,
204 preventing pR-ubiquitination of target proteins or the generation of pR-Ub. The consequent

ADPr-modified polyubiquitinated structures are resistant to DUB attack (Fig. 2A), allowing interrogation of Ub modification without confounding Rtn4 rearrangements. To analyze the consequences of *L. pneumophila* derivatives altered in Sde family function, BMDM monolayers were challenged for 20 min, and changes in polyUb about the LCV were analyzed by probing fixed samples with a polyUb-specific antibody (Fig. 2B). Neither *sdeC*$_{C118S}$ (DUB^{-}) nor *sdeC*$_{E859A}$ (ART^{-}) mutants showed significant increases in polyUb fluorescence intensity/vacuole if the analysis were restricted to LCVs having associated polyUb (Fig. 2B). In contrast, challenge with the *L. pneumophila* PDE^{-} mutant resulted in dense accumulation of LCV-associated polyubiquitination in spite of the fact that Rtn4 rearrangements were blocked (Fig. 2B). This dense association was maintained over time (Fig. 2C). Most notable was the presence of unusual polyUb-modified structures after challenge with the PDE^{-} mutant. While the Δ*sde* and ART^{-} mutants showed polyUb staining about individual LCVs (Figs. 2E,G), the PDE^{-} mutant showed polyUb structures that wrapped around the LCV and extended into serpentine structures across the interior of the BMDM (Fig. 2H). We occasionally observed dense structures in response to challenge with the DUB^{-} mutant as well (Fig. 2F), but the frequency was little changed from WT (Figs. 2B,C). We conclude that Sde-mediated modification of polyUb chains stabilizes LCV-associated Ub from the attack by both bacterial- and host derived DUBs. The observed deregulation of associated polyubiquitination in the absence of PDE activity indicates that direct modification of Ub is sufficient to stabilize polyUb. Furthermore, there is no evidence that pR- or ADPr-Ub modification plays a role in blocking polyubiquitination.

Sde-mediated modification of polyUb blocks autophagy adaptor SQSTM1/p62 binding via UBA domain.

The Ub Arg42 residue is a key target for modulating ubiquitin dynamics. Autophagy adaptors such as p62 link ubiquitinated compartments to LC3-decorated phagophores via ubiquitin associated (UBA) domains that recognize a hydrophobic patch on the Ub surface[50, 51].

231 Integral to this patch are the residues I44, V70 and L71, directly proximal to R42, the target
232 residue of ADPr modification by Sde (Fig. 3A, blue arrows). Structural analysis has shown that
233 R42 can directly participate in the UBA interface (Fig. 3B) and is likely involved in p62
234 recognition based on NMR analysis[52, 53]. We therefore tested if modification of the Ub at Arg42
235 residue blocks recognition by the p62 autophagy adaptor.

236 His-p62-Ni-NTA resin was challenged with K48- or K63-linked Ub_{3-7} mixed polymers
237 that had been pretreated with SdeC WT or its catalytic mutant derivatives (Materials and
238 Methods). The unbound fraction was collected (FT; flow through), and the p62-associated Ub_{3-7}
239 (Eluate) was detected after co-elution with imidazole, followed by SDS-PAGE fractionation and
240 immunoprobing with anti-Ub (Fig. 3C). In the absence of SdeC, both K48- and K63-linked Ub_{3-7}
241 were efficiently co-eluted with p62 (Fig. 3D; no SdeC preincubation). In contrast, pretreatment
242 with the SdeC WT, DUB^- (C118S) or PDE^- (H416A) derivatives all reduced K63- or K48-linked
243 Ub_{3-7} binding to p62 (Fig. 3D; E lanes). This indicates that either pR- or ADPr-modification of
244 polyUb blocks p62 recognition. In the case of the K48 derivative, the loss of the ART domain
245 restored Ub_{3-7}-p62 coelution, however it caused depolymerization of K48-linked Ub_{3-7} into
246 monomeric Ub, making the effects of this mutant difficult to evaluate in this assay (Fig. 3D;
247 E859A).

248 To determine the effects of Ub Arg42 modification in a more quantitative assay, binding
249 affinities to Ub_4 were determined using surface plasmon resonance (SPR) in the presence of a
250 DUB inhibitor (Ub-propargylamide, Ub-PA) to prevent degradation of the Ub_4 polymer (Fig.
251 S2A). K63-linked Ub_4 was modified by SdeC WT or its catalytic mutant derivatives in the
252 presence of Ub-PA (Materials and Methods), the modified K63-linked Ub_4 was introduced onto
253 flow chips with immobilized p62, and binding was measured by SPR over time (Fig. 3E). In the
254 absence of SdeC, Ub_4 bound His-p62 with apparent K_D~1 X 10^{-7} M, indicating that binding
255 affinity was at least as efficient as previous SPR studies using diUb as a substrate (K_D = 9.3 X 10^{-}
256 ^{8} M; [54]) (Fig. 3F). Binding of p62 to mono-Ub was very poor, consistent with DUB activity

interfering with recognition of p62 (Fig. 3G, Fig. S2C). Ub_4 pretreated with SdeC, either in the presence of Ub-PA or having the C118S DUB mutation, resulted in blockade of p62 binding, consistent with phosphoribosylation blocking recognition of Ub by UBA domains (Figs. 3H,I). ADPr modification of Ub at Arg42 was sufficient to block binding, as the $SdeC_{H416A}$ PDE^- mutant blocked binding as efficiently as WT (Fig. 3J). Elimination of the ART activity restored Ub_4 binding to p62, with a similar binding affinity to untreated, consistent with PA blocking the DUB activity (Fig 3K; $K_D = 1.6 \times 10^{-7}$ M). These results strongly argue that modification of the Ub at Arg42 residue by SdeC disrupts recognition by p62.

Sde-mediated modification of polyUb chains prevents association of p62 with the LCV.

To determine if Sde proteins enzymatically camouflage the replication vacuole from recognition by p62, BMDMs were challenged with *L. pneumophila sde* variants and probed for p62 localization about the LCV. A variety of p62 morphological variants were observed. After bacterial contact (5 min centrifugation) and immediate fixation, LCVs harboring *L. pneumophila* WT were free from the punctate localization of p62 found throughout the cytoplasm (Fig. 4A). In contrast, a large fraction of the vacuoles after challenge with the *L. pneumophila* Δ*sde* strain were enveloped by p62 (Fig. 4B). As time progressed, a variety of morphologies became apparent, such as the alignment of puncta proximal to the LCV. As puncta associated with the LCV were difficult to distinguish from those in the general vicinity, we limited quantification to identifying vacuoles with enveloping p62 structures and determining total p62 intensity associated with individual vacuoles.

Immediately after bacterial contact with BMDMs, both the WT and the $T4SS^-$ strains were devoid of p62 staining (Fig. 4C). In contrast, approximately 30% of the *L. pneumophila* Δ*sde* bacteria were found to be enveloped by p62 (Fig. 4C). Colocalization was largely lost when either *sdeA, sdeB, or sdeC* expressed on plasmids was introduced into the Δ*sde* strain. Quantification of p62 signal associated with the LCV showed that there were two populations of bacteria after challenge with the Δ*sde* strain, with a population showing p62 recruitment levels that were similar

284 to WT and a second population with 8-10X higher fluorescence intensity (Fig. 4D). In contrast,
285 the WT and Δ*sde* strains harboring Sde isoforms *in trans* showed indistinguishable low levels of
286 p62 recruitment (Fig. 4D).

287 As the infection proceeded, colocalization of p62 with the Δ*sde* strain continued to
288 increase (Fig. 4E, >50% at 20 MPI) with the population of LCVs strongly skewing toward
289 hyperaccumulation of p62 (Fig. 4F). Concurrently, a second phenomenon became apparent in
290 strains harboring plasmids that produced excess Sde isoforms. There was clear complementation
291 of the Δ*sde* defect (Fig. 4E), but accumulation of p62 about the LCV at 20 MPI was observed
292 that distinguished these constructs from the WT strain (Fig. 4E). Accumulation could also be
293 observed when the fluorescence intensity of individual LCVs was determined, with a population
294 emerging with increased p62 density (Fig. 4F). This phenomenon appeared to be a premature
295 version of what occurs with the WT strain, as 20% of the LCVs harboring the WT showed
296 accumulation of p62 by 60 MPI, with evidence of an emerging population showing increased
297 p62 density about the LCV (Figs. 4G, H). There was robust accumulation of p62 about
298 individual LCVs harboring WT strain at this timepoint that appeared indistinguishable from
299 individual LCVs harboring the Δ*sde* strain (Fig. 4I). Furthermore, at 180MPI, accumulation of
300 p62 around the LCV in the Δ*sde* strain was indistinguishable from p62 accumulation around WT
301 LCVs (Figs. 4J, K). When the percentage of LCVs associated with p62 was plotted as a function
302 of time post-infection (Fig. 4L), there was early accumulation of p62 that was blocked by the Sde
303 family (0-20 MPI). This was followed by decay of p62 accumulation after infection of the Δ*sde*
304 strain, while the WT showed increasing p62 between 20 and 60 MPI, resulting in a convergence
305 of the phenotypes (180 MPI). The loss of Sde protection of the LCV is consistent with reversal
306 of its activity by known metaeffectors SidJ and DupA/B [24, 25, 26, 55].

307 To determine the role of the individual Sde activities in preventing p62 accumulation,
308 point mutations in each of the three catalytic domains were analyzed at 0 MPI after macrophage
309 challenge, when the Sde family exerts its most striking effects. Mutations in *sdeB* were introduced
310 into the Δ*sde* strain, as this isoform showed the most effective complementation (Fig. 4C), and

311 these mutants were then used to challenge macrophages. Point mutations in the catalytic sites of
312 the DUB or PDE domains, as well as a double mutant missing the catalytic activity in both of
313 these domains, still retained the ability to block p62 colocalization after association (Figs. 5A-C).
314 In contrast, a mutation in the ART domain caused a large increase in p62 recruitment to LCVs,
315 indicating that ADP ribosylation of Ub Arg42 by the ART domain blocks p62 recognition of the
316 LCVs (Fig. 5A). It should be noted that there appeared to be some residual interference of p62 in
317 the single ART mutant, but this was eliminated by simultaneously introducing a DUB mutation,
318 indicating that the DUB domain may play a minor role in lowering p62 recognition of the LCV
319 (Fig. 5A). As seen with the Δ*sde* strain, the ART mutants resulted in a clear subpopulation
320 showing approximately 10-fold increase in p62 accumulations (Figs. 5B,C). These results support
321 the biochemical data that either ADPribosylation or phosphoribosylation of Ub at Arg42 is
322 sufficient to block p62 recognition. It also argues against models that propose pR-linked Ub
323 modification of a peripheral factor plays a role[56], as ADPribosylation of Ub was sufficient to
324 interfere with p62 recruitment.
325

Discussion.

The *L. pneumophila* Sde family drives phosphoribosyl-linked ubiquitination (pR-Ub) of targets, most spectacularly leading to largescale rearrangements of the tubular ER protein reticulon 4 (Rtn4)[22]. In addition, there are two accessory activities of Sde proteins that have unclear biological roles. The Sde deubiquitinase (DUB) domain preferentially deubiquitinates Lys63-linked polyubiquitin chains (Fig. 1)[32], while the other is the hydrolytic product of ADPribosylated ubiquitin (ADPr-Ub), resulting in phosphoribosylated ubiquitin (pR-Ub)[22, 57]. The phosphoribosylation occurs at the Ub Arg42 residue, strategically placed in a hydrophobic patch that provides a recognition surface for ubiquitin binding proteins that drive autophagy (Fig. 3A,B)[52, 58]. The presence of Sde family members is linked to a lowered association of Ub-recognizing autophagy adaptors to the LCVs[48], consistent with phosphoribosylation promoting maintenance of the LCV in the face of cytosolic antimicrobial attacks.

In this manuscript, we showed that inhibition of polyUb formation about the replication vacuole was transiently controlled by the Sde DUB domain and limited to the earliest times after infection (Fig. 1). This early degradation of polyUb by the DUB domain fueled phosphoribosyl-linked ubiquitination because pR-Ub modification of Rtn4 slowed greatly in the absence of DUB activity and was accompanied by a reduction in Rtn4 accumulation about the replication vacuole (Fig. 1D-M). Therefore, it appears that there is K63-polyubiquitination of the LCV about the nascent replication vacuoles[39, 59, 60, 61, 62, 63] that provides the substrate for the Sde DUB activity, generating monoubiquitin fuel for the Sde mART domain (Fig. 6B,C). This is then directly transferred by the PDE domain to generate pR-Ub modified Rtn4, allowing a direct pathway from vacuolar polyUb to endoplasmic reticulum (ER) rearrangements (Fig. 6D).

The association of polyUb with the replication vacuole should be a suicide signal for *L. pneumophila*, as ubiquitination marks intracellular compartments for degradation by the autophagy pathway[45, 64]. Autophagy results from binding of adaptor molecules (such as p62) to Ub-modfied compartments which, in turn, bridge to autophagophores decorated by LC3/Atg8[65]. It is well established that after *L. pneumophila* forms the LCV, autophagy is blocked via the action

353 of the Icm/Dot substrate RavZ, which irreversibly hydrolyzes and deconjugates LC3/Atg8 from
354 the nascent autophagophore, blocking binding to autophagy adaptors[46]. In the absence of RavZ,
355 the LCV is still resistant to autophagy, indicating that the vacuole is masked in a fashion that
356 prevents recognition by the LC3-decorated autophagophore[46, 48]. We show here that modifying
357 the Arg42 residue of polyUb with either mono-ADPribose or phosphoribose physically blocks
358 binding to the autophagy adaptor p62 (Fig. 3), and similar results have been obtained by Wan and
359 coworkers[49]. Surface plasmon resonance experiments showed no detectable p62 binding in
360 presence of high concentrations of polyUb modified by either WT (pR modification) or the
361 H416A derivative (ADPr modification; Fig. 3F-K). Consistent with the data using purified
362 proteins, both modifications blocked p62 association with the LCV (Fig. 5) and stabilized polyUb
363 about the replication vacuole (Fig. 2). In fact, the ADPr modification resulted in
364 hyperaccumulation of polyUb about the replication vacuole (Fig. 2B,C), consistent with enhanced
365 resistance to both DUBs and autophagy adaptor recognition.
366 That all the proposed functions of phosphoribosylation can be fulfilled without hydrolysis
367 of the ADPr modification questions the purpose of the pR modification. It seems likely that
368 allowing vacuole-associated polyUb to accumulate ADPr modifications would result in covalent
369 linkage of Sde targets directly to the replication vacuole, even if this is a low likelihood event [22,
370 27, 34]. In addition, the ART and PDE domains work independently and consecutively, allowing
371 ADPr modification to persist on polyubiquitin chains, raising the possibility that unwanted
372 proteins would be immobilized about the replication vacuole. This problem is particularly
373 exacerbated by the fact that Sde-promoted pR-Ub linkage preferentially occurs on unstructured
374 regions of proteins, which could drive promiscuous linkage of poorly folded proteins about the
375 vacuole. Therefore, hydrolysis of ADPr-Ub at Arg42 acts as a timing device, requiring target to
376 be immediately accessible to Sde and ADPr-Ub prior to decay to pR-Ub.
377 It has been previously reported that pR-Ub modification of USP14, a host cell
378 deubiquitinase, is a central strategy for preventing p62 association with the *Legionella* replication
379 vacuole[56]. The authors proposed that modification of USP14 disrupted its direct interaction with

380 p62, preventing association of the LCV with the autophagy adaptor[56]. The data we presented here
381 argue against USP14 modification being a major mechanism for autophagy avoidance, and that
382 modification of LCV-associated Ub is likely the primary strategy used by Sde proteins to protect
383 against autophagy. First, pR-modification of Ub blocked p62 association (Fig. 3), and, given the
384 expected stoichiometry of Ub relative to USP14, it is likely that this direct blockade is the primary
385 contributor to autophagy avoidance. Secondly, ADPr-modification of poly-Ub was sufficient to
386 avoid autophagy (Figs. 2B, 5A), arguing that pr-Ub modifications of any peripheral targets such
387 as USP14 are unlikely to contribute to autophagy avoidance. Finally, we showed that there was a
388 minor, but detectable, contribution of the DUB domain to autophagy avoidance (Fig. 5A),
389 consistent with host DUBs making similar enzymatic contributions, rather than playing a role in
390 direct binding to the p62 target.

391 Our data on the transient nature of p62 blockade illustrates an important biological
392 principal underlying Sde family function (Fig 4L). There is little, if any, association of p62 with
393 the *L. pneumophila* WT replication vacuole during the first 20 minutes of macrophage infection.
394 In contrast, challenge with the Δ*sde* strain results in p62 association with the LCV at early
395 timepoints (Figs. 4E,L). This huge difference largely disappears by 1 hour post infection, as there
396 appears to be increased accumulation of p62 about the WT LCV, with coordinate decreased p62
397 accumulation about the Δ*sde* LCV (Fig. 4L). By 3 hr post infection, the Δ*sde* mutant and WT look
398 indistinguishable, with each showing about 80% of the LCVs devoid of p62 localization.
399 Therefore, function of Sde decays rapidly during the first hour after infection, with a new activity
400 appearing in both strain backgrounds that interferes with p62 association.

401 The decay in protection from p62 association is predicted by the function of proteins that
402 modulate Sde family activity. Icm/Dot translocated proteins SidJ and SdjA glutamylate Sde
403 proteins, blocking their ability to ADPribosylate ubiquitin[23, 24, 25, 26]. As expression of the *sde*
404 genes appears to be downregulated after contact with mammalian cells[19, 66], this modification
405 effectively removes the pool of enzyme capable of ADPribosylating Ub. The fact that over time
406 there is some increase in the level of p62 association with the WT LCV indicates that there is

407 accumulation of polyubiquitin about the LCV during the first hour after infection that cannot be
408 modified by the inactivated Sde enzymes. In this regard, it should be noted that pR-Ub
409 modification of target proteins is also reversed by the linkage-specific deubiquitinases DupA and
410 DupB, consistent with a general decay in Sde function as well as loss of memory of its activity
411 during the first hour after infection[27, 28]. Therefore, Sde functions as critical cog in the
412 morphogenesis of the LCV during the earliest stages of replication vacuole establishment.
413 Efficient intracellular growth requires decay in Sde function, as SidJ mutants that result in
414 extended Sde family activity show slowed intracellular growth[67].
415 In summation, the Sde family is involved in critical early steps that are associated with
416 homeostatic regulation of replication vacuole morphogenesis. Accessory activities that modulate
417 polyubiquitin dynamics about the replication vacuole are tightly linked to phosphoribosyl-linked
418 ubiquitination of substrate (Fig. 6). We argue that the DUB domain provides fuel for pR-Ub
419 modification, while pR modification of polyubiquitination about the LCV prevents attack by an
420 important arm of host cell cytosolic defense. Finally, the transient nature of Sde function during
421 replication vacuole formation is an intrinsic feature of this system, as we witness decay in the
422 ability to block the autophagic response. The transient nature of providing fuel for Sde function is
423 also supported by this work, as phosphoribosyl modification of polyUb is predicted to block DUB
424 function (Fig. 2) and reduce the amount of fuel to support Sde-mediated ubiquitination of
425 substrates. The biological importance of limiting Sde function to the earliest stages of replication
426 compartment biogenesis requires further investigation.
427

Materials and Methods

Bacterial culture and media

L. pneumophila derivatives used in these studies were streptomycin-resistant restriction-defective thymidine auxotrophs derived from a clinical isolate of *Legionella pneumophila*, strain Philadelphia-1 (Lp01)[11, 68, 69]. *L. pneumophila* strains were propagated on charcoal–N-(2-acetamido)-2-aminoethanesulfonic acid (ACES)–yeast extract plates, with or without thymidine as needed (CYE/T) and in ACES-yeast extract broth (AYE/T)[7, 11, 70]. Plasmids were introduced as described[22].

For the infection of mammalian cells, *L. pneumophila* strains were grown overnight to post-exponential phase (OD_{600} 3.5-4.5) to a predominantly motile state as described previously[71]. Strain derivatives are described in Supplemental Table 1 and oligonucleotides used in this study are listed in Supplemental Table 2.

Eukaryotic cell culture

Bone marrow-derived macrophages (BMDMs) were isolated from femurs and tibias of female 6-10week old A/J mice[7] and frozen in fetal bovine serum (FBS) with 10% dimethyl sulfoxide (DMSO). Cells were plated the day before infection in RPMI 1640 (Gibco) supplemented with 10% FBS and 2 mM glutamine at 37°C with 5% CO_2. HEK293T cells, obtained from ATCC, were cultivated in Dulbecco modified Eagle medium (Gibco) supplemented with 10% heat-inactivated (FBS, Invitrogen) (vol/vol), 100U/ml of penicillin-streptomycin (Gibco) at 37°C with 5% CO_2.

Polyubiquitin colocalization with LCV

BMDMs were plated on glass coverslips at 1-2 x 10^5/well in 24-well plates. Cells were challenged at a multiplicity of infection (MOI) = 1, centrifuged at 200 x g for 5 min and incubated for the indicated time points. The infection mixtures were then fixed in PBS

containing 4% paraformaldehyde, permeabilized in PBS containing 1% (vol/vol) Triton X-100 for 30 min, probed with mouse anti-polyUb (Enzo Life Biosciences, Cat# BML-PW8805-0500, 1:250) and rabbit anti- *L. pneumophila* followed by secondary probing with goat anti-rabbit Alexa Fluor 594 (Invitrogen, Cat# 111-585-144, 1:500) and donkey anti-mouse Alexa Fluor 488 (Jackson ImmunoResearch, Cat# A-11012, 1:500). Hoescht 33342 (Life Technologies, Cat#62249 1:10,000) was used to label nuclei.

Immunofluorescence of Rtn4-LCV colocalization

BMDMs were plated on glass coverslips at 1-2 x 10^5/well in 24-well plates. Cells were infected at a multiplicity of infection (MOI) = 1, centrifuged at 200 x g for 5 min and incubated for 1 hr. The infection mixtures were then fixed in PBS containing 4% paraformaldehyde, permeabilized in PBS containing 1% (vol/vol) Triton X-100 for 30 min, probed rabbit anti-RTN4 (Lifespan Biosciences, Cat# LS-B6516, 1:500) and rat anti- *L. pneumophila*[72] followed by secondary probing with goat anti-rabbit Alexa Fluor 488 (Jackson ImmunoResearch, Cat# 111-545-003, 1:500) and donkey anti-rat Alexa Fluor 594 (Jackson ImmunoResearch, Cat# 712-585-153, 1:500). Hoescht 33342 (Life Technologies, Cat#62249 1:10,000) was used to label nuclei.

Rtn4 Immunoprecipitations

For transfections preceding Rtn4 Immunoprecipitations (IP), HEK293T cells were plated in DMEM medium containing 10% fetal calf serum at a density of 4 x 10^6 cells in a tissue culture-treated 10cm dish. The next day, 12µg of pMT123 DNA (pHA::ubiquitin) was transfected into cells using Lipofectamine 2000, following manufacturer's procedure (Life Sciences). The mammalian HA::ubiquitin expression plasmid pMT123 was a kind gift from D. Bohmann and S. Lippard[59, 73]. The next day, transfection medium was removed and replaced with DMEM with 10µM MG132 (Calbiochem) at ~30-60min prior to challenge with *L. pneumophila* at an MOI=10 for the indicated times. Post infection, cells were lifted and washed

in PBS, centrifuged at 4°C at 200 x g, and then cell pellets were immediately frozen on liquid nitrogen and stored at -80°C until used[22].

For immunoprecipitations, anti-Rtn4 resin was generated by disuccinimidyl suberate crosslinking with anti-Rtn4 (Nogo N-18, Santa Cruz sc-11027) to Protein A/G Plus™ resin at 2µg/µl of packed resin as described in manufacturer protocol (Pierce crosslink IP kit). Samples were lysed in 1% Triton X-100 (20 mM Tris [pH 7], 150 mM NaCl, 5 mM $MgCl_2$) containing protease inhibitor (Roche, Cat# 11697498001) with end-over-end rotation for 20 min at 4°C. Cleared cell lysates were obtained by centrifugation at ≥14,000 x g for 10 min at 4°C, diluted with an equal volume of detergent-free buffer, and mixed with washed resin (50% slurry). The mixture was incubated at 4°C via end-over-end rotation for ≥ 4 hr, then washed ≥ 5X in the buffer containing 0.1% Triton X-100 at 4°C.

For elution, Rtn4 resin in spin columns was incubated with 0.1M glycine (pH = 2.8) with 0.2% Triton X-100 for 5min, centrifuged, then eluate was reapplied to resin for additional 5 min incubation at room temperature, centrifuged and neutralized with 0.5M Tris (pH=10.55)[22]. Eluate bound to resin was resuspended with reducing SDS sample buffer, boiled, then fractionated by SDS-PAGE coupled with immunoblot analyses.

Protein purification

Full-length *sdeC* genes were amplified by PCR and cloned into the bacterial expression vector pQE-80L (Qiagen) with *BamHI* and *SacI* restriction sites to generate a 6xHis-SdeC-StrepII fusion construct (Supplemental Table 1). Purification was as previously described[22]. Purified aliquots were stored at -80°C in 10% glycerol to minimize or eliminate freeze thaw cycle degradation.

Deubiquitinase assay in presence of Sde modification

His-tagged recombinant SdeC and its derivatives were bound to Ni-NTA (Thermo Fisher Scientific, Cat# 88221) resin at 1 µg enzyme per 25µl of packed resin in 1X ART buffer (20mM

508 Tris 10mM NaCl, pH7.4) for 1 hr at 4°C with end-over-end rotation. The beads were washed 3X
509 with 1X ART buffer to remove non-adsorbed enzyme with microcentrifuge spin filters spun at
510 3000 x g at room temperature. After the final wash, each 25µl of pelleted resin was incubated
511 with 2µg of recombinant human K63-linked (R&D systems, Cat# UC-320) or K48-linked (R&D
512 Systems, Cat# UC-220) poly-ubiquitin and 500µM ε-NAD in 300 µl of 1X ART buffer for 2 hrs
513 with end-over-end gentle rotation at 37°C. After incubation, the SdeC or its derivatives-bound
514 resin were removed with microcentrifuge spin column filters, and the polyUb reaction mixture
515 was collected. This polyUb fraction was then incubated with either 1) 100 nM human
516 recombinant PolyHistidine-otubain 1(R&D systems, Cat# E-522B), 2) 50 nM recombinant
517 USP2 catalytic domain (R&D systems, Cat# E-504), 3) 50 nM recombinant PolyHistidine-
518 CYLD (R&D systems, Cat# E-556), or 50nM recombinant SdeC DUB (1-192) at 37°C in 1X
519 ART buffer for 2 hr. A fraction of the reaction was removed, terminated by the addition of
520 reducing sample buffer, and then heated to 50-55°C for 20-30min to avoid Ub chain aggregation.
521 Relative DUB activity was determined by immunoblot probing of SDS- SDS-PAGE fractionated
522 proteins using Image Studio software (LI-COR Biosciences) after 2 hr incubation by comparing
523 the efficiency of cleavage of modified Ub relative to unmodified.
524

525 **Immunoblotting**

526 Immunoblots were performed as described [74]. Samples were fractionated by SDS-PAGE
527 and transferred to nitrocellulose membranes. The membrane was blocked in 50 mM Tris-
528 buffered saline with 0.1% Tween-20 (TBST, pH 8.0) containing 4% nonfat milk for 1 hr at room
529 temperature and probed with primary antibodies: 1) anti-HA-probe (Santa Cruz Biotechnology,
530 Cat# sc-7392, 1:500), 2) anti-Ub (Santa Cruz Biotechnology, Cat# sc-8017) or anti-actin (Sigma-
531 Aldrich, Cat# A2066, 1:1,000) in TBST containing 2% BSA at 4°C overnight. After washing 3X
532 with TBST, the membranes were incubated with secondary antibodies: donkey IRDye 680RD
533 anti-mouse (LI-COR Biosciences, Cat# 926-68072, 1:20,000), Goat IRDye 680RD anti-rabbit

534 (LI-COR Biosciences, Cat# 926-68071, 1:20,000), and/or donkey IRDye800CW anti-mouse (LI-
535 COR Biosciences, Cat# 926-32212, 1:20,000), goat IRDye 800CW α-rabbit (LI-COR
536 Biosciences, Cat# 926-32211, 1:20,000) for 45 min at room temperature. Capture and analysis
537 were performed using Li-Cor Odyssey CLX scanner and Image Studio software (LI-COR
538 Biosciences).
539

540 **Bead-binding assay for adaptors association with polyUb post Sde-mediated modification**
541 **of Ub**

542 His-tagged recombinant full-length SdeC derivatives were adsorbed to Ni-NTA (Thermo
543 Fisher Scientific, Cat# 88221) resin at 1µg enzyme per 25 µl of packed resin in 1X ART buffer
544 for 1 hr at 4°C with end-over-end rotation. The SdeC adsorbed resin was washed 3X with 1X
545 ART buffer to remove nonadsorbed enzyme with microcentrifuge spin filters centrifuged at 3000
546 x g at room temperature. After the final SdeC resin wash, each 25 µl pelleted resin was
547 resuspended with 4µg of recombinant human homotypic-linked polyubiquitin chains Ub_{3-7} (K63
548 or K48, 4µg/600µl reaction volume, Boston Biochem, R&D) and 500µM ε-NAD in 1X ART
549 buffer for 2 hrs with gentle end-over-end rotation at 37°C. During incubation of SdeC and
550 polyUb chains, 1µg recombinant PolyHis-p62 was adsorbed to 5 µl pre-equilibrated packed Ni-
551 NTA resin (Thermo Fisher Scientific, Cat# 88221) via 1 hr, end-over-end rotation at 4°C in low
552 adhesion 1.5 ml microcentrifuge tubes. Polyubiquitin chains were then separated from SdeC by
553 collection of SdeC resin in a microcentrifuge column spin filter and then the polyUb fraction was
554 incubated with recombinant PolyHis-p62 on Ni-NTA resin for 1 hr at room temperature with
555 end-over-end rotation. The resin was washed 3-5X with 50mM Tris 0.1% BSA (vol/vol) pH7.5
556 at room temperature, then resin having adsorbed proteins and bound polyUb chains were eluted

from the Ni-NTA beads with 250 mM imidazole diluted in 50 mM Tris 0.1% BSA (vol/vol) pH7.5. Samples were then analyzed by SDS-PAGE followed by immunoblot.

SPR analysis of Sde-mediated modification on binding of poly-Ub to p62

For modification of Ub, 100 µg of K63-linked Ub tetramer (R&D Systems, Cat# UCB-310) or monomeric Ub were incubated together with 100 µM β-NAD and 20 nM SdeC variants (WT, C118S/DUB$^-$, E859A/ART$^-$ and H416A/PDE$^-$) in 250 µl of 1X ART buffer at 37°C for 1 h. For DUB inhibitor pretreatment, 1 µM ubiquitin-propargylamide (R&D Systems, Cat# U-214) was incubated with 100 nM SdeC variants at room temperature for 30 min before adding to Ub_4 (final concentration, 20 nM SdeC in 1X ART buffer). To remove the SdeC, 10 µl of a 50% slurry of Ni-NTA agarose resin (Thermo Fisher Scientific, Cat# 88221) was washed three times with 1X ART buffer, then added to the Ub-SdeC reaction for another 1hr with end-over-end rotation at 37°C. For removal of SdeC enzyme, the samples were centrifuged at 1000 x g for 2 min in a microcentrifuge spin filter column. The supernatant was then desalted using a NAP-5 column (Thermo Fisher Scientific, Cat# 45-000-151) and lyophilized with a Labconco Freezone12. Samples were resuspended in Ultrapure water to a final protein concentration of 1 mg/ml.

The binding kinetics between p62 and modified Ub_4 was determined by surface plasmon resonance (SPR) using a Biacore T200 system, with a runner buffer of HEPES Buffered Saline (HBS; 10 mM HEPES (pH =7.4), 150 mM NaCl) containing 30 µM of EDTA. 6xHis-tagged p62 was captured onto a Series S NTA sensor chip following manufacturer's recommendations (Cytiva, Cat# 28994951). Briefly, 0.5 mM $NiCl_2$ solution was injected at a flow rate of 10 µl/min for 60 seconds onto the experimental flow cell, followed by the injection of His-p62 (200 nM) at 5 ul/min for 420 seconds. Ub_4 at various concentrations, that had been previously treated with

SdeC derivatives, was injected into the flow cells at a rate of 30 µl/min for 180 seconds, followed by a 300 seconds dissociation phase. Regeneration of the surface was performed by two injections of 350 mM EDTA (30 ul/min, 60 seconds) followed by an injection of 6M guanidine hydrochloride with 50 mM NaCl (30 ul/min, 30 seconds). The binding kinetics were determined with Biacore Evaluation software (v3) using double referenced sensorgrams and 1:1 binding for the fitting model.

Immunofluorescence of p62 at the LCV

BMDMs were plated on glass coverslips at 1-2 x10^5/well in 24-well plates. Cells were challenged at a multiplicity of infection (MOI) = 2, centrifuged at 200 x g for 5 min, and incubated for the indicated time points. For 180 min infections, the cells were washed 3X in PBS at 60 min post-infection to remove non-internalized bacteria, then fresh culture media was added. At the infection conclusion, all cells were washed 3X in PBS, fixed in PBS containing 4% (wt/vol) paraformaldehyde, followed by permeabilization with ice-cold 100% methanol for 20 seconds. Coverslips were then washed 3X in PBS and blocked in PBS containing 2-4% BSA for at least 30 min. Cells were then stained in PBS with rat anti-*L. pneumophila* and rabbit anti-p62/SQSTM (Abcam, Cat# 109012, 1:400) for 1 hr and detected with donkey anti-rat Alexa Fluor 594 (Jackson ImmunoResearch, Cat# 712-585-153, 1:500) and goat anti-rabbit Alexa Fluor 488 (Jackson ImmunoResearch, Cat# 111-545-003, 1:500). Hoechst 33342 was used to label DNA.

Image analysis

Representative images were taken using Zeiss Axiovert or Nikon inverted phase fluorescence microscopes, and image enhanced in Photoshop™ (Adobe), using linear corrections. For quantification of total polyUb intensity, Volocity software (PerkinElmer) was used. ROIs (regions of interest, 14 x 12 µm; oval) were set around LCVs, and pixel intensities were measured and subtracted by background intensity. For quantification of total p62 intensity,

we set ROIs (0.3 x 0.42 inches; oval) around LCVs. Mean p62 intensity/pixel was measured in each ROI and subtracted by background intensity/pixel using Fiji image analysis software[75].

Acknowledgements. K.K. was supported by NIH training grant T32GM007310. This work was supported by NIAID grants R01AI113211 and R01AI146245 to R.I. Panels 3A and 3B were used under terms of Creative Commons. We thank Drs Kevin Manera and Atish Roy Chowdhury for review of the manuscript and Dr. Yuxin Mao for communication of results before publication.

Figure Legends

Figure 1. The Sde DUB domain is required for efficient phosphoribose-ubiquitination of Rtn4.

(A) Domain structure of Sde family proteins. Catalytically inactive point mutations are shown in red. **(B, C)** Percent poly-Ub positive LCVs of *L. pneumophila* strains at noted timepoints post-infection. **(D, E)** Quantification of Rtn4-positive LCVs. BMDMs were challenged with indicated strains for the noted infection times, followed by fixation, permeabilization with 1% Triton X-100 and probing as described in Materials and Methods. 0 MPI was immediately after 5 min centrifugation of bacteria onto BMDM. Noted strains are wild type, Lp02; Δ*sde*, Δ*sidE*Δ*sdeC*Δ*sdeB-A*; Δ*sdeC-A*, Δ*lpg2153-2157* (KK034), listed in Supplemental Table 1. At least 150 LCVs per experiment were evaluated and data were pooled from 3 biological replicates (mean ± SEM; one-way ANOVA with Dunnett's multiple comparison **(B, C)** and Student's t-test **(D, E)**; ns (non-significant), *p<0.05, **p<0.01, ***p<0.001, ****p < 0.0001). **(F-K)** A representative micrograph of Rtn4 recruitment, scale bar 5 µm. Macrophages were challenged with either WT or noted mutant strains for 1 hr, fixed, permeabilized and probed with anti-*L. pneumophila* (Alexa Fluor 594 secondary, red), anti-Rtn4 (Alexa Fluor 488 secondary, green), and Hoechst (nucleus, blue). **(L)** Cartoon of strategy to identify pR-Ub modified Rtn4. **(M)** Immunoblot image of anti-Rtn4 immunoprecipitates by immunoprobing with anti-HA. To right of immunoblots are Rtn4 isoforms and modification status. HEK293T cells were challenged with noted *L. pneumophila* strains for either 10 or 180 mins. Modified Rtn4 substrates were immunoprecipitated using crosslinked anti-Rtn4, fractionated on 7.5% SDS-PAGE, and probed with anti-HA. Lanes: WT, Lp02; vector, Δ*sde*; p*sdeA*, Δ*sde* expressing SdeA; p*sdeA C118S*, Δ*sde* expressing SdeA DUB mutant; p*sdeB*, Δ*sde* expressing SdeB; p*sdeB C118S*, Δ*sde* expressing SdeB DUB mutant; MOCK, uninfected.

Figure 2. The ART domain blocks DUB activity and promotes hyper-polyubiquitination of the LCV.

(**A**). SdeC WT or its catalytic mutant derivatives (1μg) were adsorbed to Ni-NTA resin for 1 hr at 4°C, then incubated with either K63 or K48-linked polyUb$_{3-7}$ (2μg) for 2 hrs at 37°C. SdeC resin was removed and polyUb$_{3-7}$ was then incubated with: human recombinant Polyhistidine-otubain 1, isoform 1 (100 nM); recombinant USP2 catalytic domain (50 nM); recombinant Polyhistidine-CYLD (50 nM); or recombinant SdeC DUB CD 1-192 (50 nM) at 37°C for 2 hrs. Cleavage was monitored by immunoblotting with anti-Ub (FK1). (**B**) Quantification of polyUb intensity associated with individual LCVs of the noted strains at 20 MPI. **(C)** PolyUb intensity of LCVs harboring Δ*sde* expressing SdeC PDE^{-} (H416A) mutant at 20 or 60 MPI. Data are shown in median ± 25%ile; Mann-Whitney test; ns (non-significant), **p<0.01, ***p<0.001, ****p < 0.0001. The dotted lines represent background level of polyUb intensity about LCVs. **(D-H)** Examples of polyUb-positive LCVs. BMDMs were challenged by 5 min centrifugation at an MOI of 1, incubated with noted *L. pneumophila* strains, fixed, permeabilized with 1% Triton X100, and probed with anti-polyUb (Alexa Fluor 488 secondary, green), anti-*L. pneumophila* (Alexa Fluor 594 secondary, red), and Hoechst (blue). Strains used: WT, Lp02; *Δsde*, *ΔsidE ΔsdeC ΔsdeB-A; Δsde psdeC$_{WT}$*, Δ*sde* expressing SdeC WT; *Δsde psdeC$_{C118S}$*, Δ*sde* expressing SdeC DUB mutant; *Δsde psdeC$_{E859A}$*, Δ*sde* expressing SdeC ART mutant; *Δsde psdeC$_{H416A}$*, Δ*sde* expressing SdeC PDE mutant. Scale bar: 5μm.

Figure 3. Sde-mediated modification of polyUb prevents its recognition by p62.

(A) Space filling model of Ub. R42 residue (blue letter) and I44 residue are indicated with blue arrows (from reference[52, 58]).**(B)** Interface residues between UBA domain and Ub, showing

possible involvement of Ub R42 in interacting with UBA domain (from reference[52, 58]). **(C, D)** Ub modification at R42 blocks p62 binding (Materials and Methods). Ni-NTA-p62 was incubated with Ub_{3-7} that had been treated with SdeC WT or its catalytic mutant derivatives and allowed to bind (In). Unbound Ub_{3-7} was removed (FT), the beads were washed, and then eluted with 250mM imidazole (E: elution). The p62-bound poly-Ub in the eluate was fractionated by SDS-PAGE followed by probing with anti-Ub. Relative loading: In, input (2.5%); FT, flow-through (2.5%); E, eluate (25%). (**E)** Surface plasmon resonance (SPR) quantitation of p62 binding to Ub derivatives. Ub_1 or Ub_4 was incubated with SdeC WT or its derivatives immobilized on Ni-NTA resin, the supernatant containing modified Ub derivatives was incubated with 6xHis-tagged p62 bound to a Ni-NTA chip, and binding affinity was measured by plasmon resonance. **(F, G)** Sensorgrams of Ub_4 or Ub_1 binding to p62. Binding of Ub_4 to p62 yields a $K_D = 0.97 \times 10^{-7}$ M. **(H-K)** Sensorgrams of Ub_4, modified as noted in panels (red balls: phosphoribosyl addition; green balls: ADP-ribosyl addition). Reactions were formed in the presence of Ub-propargylamide (DUB inhibitor).

Figure 4. Transient blockade of p62 recruitment to the LCV in the presence of Sde family members.

(A-B) Examples of punctate (A) or enveloped (B) p62 morphology localized around LCVs after challenge of BMDMs with noted *L. pneumophila* strains. The scale bar represents 10 µm. **(C, E, G, J)** The Percentage of circumferential p62 associated with LCVs at 0 (immediate bacterial contact; C) or 20 (E) or 60 (G) or 180 (J) MPI. 100 LCVs per replicate were counted in 3 biological replicates (mean ± SEM; one-way ANOVA with Dunnett's multiple comparison; ns (non-significant), **$p<0.01$, ***$p<0.001$, ****$p < 0.0001$). **(D, F, H, K)** Quantification of mean

p62 intensity/pixel around LCVs at 0 (D) or 20 (F) or 60 (H) or 180 (K) MPI. At least 70 vacuoles per replicate were quantified and data were pooled from 3 biological replicates (mean ± SEM; one-way ANOVA with Dunnett's multiple comparison (D, F, H) and Student's t-test (K); ns (non-significant), *p<0.05, **p<0.01, ****p < 0.0001). (**I**) A representative micrograph of p62 association with LCVs at 180 MPI, scale bar 10 µm. (**L**) Kinetics of blockade against p62 recruitment. Data acquired from panels C, E, G and J, and shown as mean ± SEM.

Figure 5. ART activity is sufficient to block p62 recruitment to the replication vacuole.

(A) Quantification of individual LCVs enveloped by p62 at 0 MPI. BMDMs were challenged with the noted *Legionella* strains. **(B)** Quantitation of mean p62 intensity/pixel associated with individual LCVs. Images of individual vacuoles were grabbed and pixel intensities of p62 staining about regions of interest were determined (Materials and Methods). 210 LCVs were counted. Data are shown as means ± SEM (one-way ANOVA with Dunnett's multiple comparison; ns (non-significant), *p<0.05, **p<0.01, ****p < 0.0001). **(C)** Examples of recruited p62 to LCVs harboring Δ*sde* expressing SdeC catalytic mutant derivatives. Scale bar: 10 µm.

Figure 6. Sde accessory activities drive Rtn4 rearrangements and block autophagic recognition.

The DUB activity provides fuel for pR-Ub modification of Rtn4, driving rapid ER-associated rearrangements. **(A)** Bacteria are internalized, Sde family proteins are translocated. **(B)** Polyubiquitination occurs about the replication vacuole. **(C)** Digestion of polyUb provides Ub fuel for ART/PDE domain to catalyze pR-Ub conjugation to substrates such as Rtn4. **(D)** Rtn4-

712 pR-Ub modified protein accumulates about the replication vacuole polyUb is modified by
713 phosphoribosylation. The pR-modification of the polyUb at R42 residue stabilizes
714 polyubiquitination about LCVs, simultaneously preventing degradation by host cell-derived
715 DUBs and blocking recognition by the autophagic machinery.
716
717

References

1. Cunha, B.A., Wu, G. & Raza, M. Clinical Diagnosis of Legionnaire's Disease: Six Characteristic Clinical Predictors. *Am J Med* **128**, e21-22 (2015).

2. Cunha, B.A., Burillo, A. & Bouza, E. Legionnaires' disease. *Lancet* **387**, 376-385 (2016).

3. Safdar, N., Crnich, C.J. & Maki, D.G. The pathogenesis of ventilator-associated pneumonia: its relevance to developing effective strategies for prevention. *Respir Care* **50**, 725-739; discussion 739-741 (2005).

4. Horwitz, M.A. & Silverstein, S.C. Interaction of the Legionnaires' disease bacterium (*Legionella pneumophila*) with human phagocytes. I. *L. pneumophila* resists killing by polymorphonuclear leukocytes, antibody, and complement. *J Exp Med* **153**, 386-397 (1981).

5. Rowbotham, T.J. Isolation of *Legionella pneumophila* from clinical specimens via amoebae, and the interaction of those and other isolates with amoebae. *J Clin Pathol* **36**, 978-986 (1983).

6. Abu Kwaik, Y. The phagosome containing *Legionella pneumophila* within the protozoan *Hartmannella vermiformis* is surrounded by the rough endoplasmic reticulum. *Appl Environ Microbiol* **62**, 2022-2028 (1996).

7. Swanson, M.S. & Isberg, R.R. Association of *Legionella pneumophila* with the macrophage endoplasmic reticulum. *Infect Immun* **63**, 3609-3620 (1995).

8. Kagan, J.C. & Roy, C.R. *Legionella* phagosomes intercept vesicular traffic from endoplasmic reticulum exit sites. *Nat Cell Biol* **4**, 945-954 (2002).

9. Horwitz, M.A. Characterization of avirulent mutant *Legionella pneumophila* that survive but do not multiply within human monocytes. *J Exp Med* **166**, 1310-1328 (1987).

10. Marra, A., Blander, S.J., Horwitz, M.A. & Shuman, H.A. Identification of a *Legionella pneumophila* locus required for intracellular multiplication in human macrophages. *Proc Natl Acad Sci U S A* **89**, 9607-9611 (1992).

11. Berger, K.H. & Isberg, R.R. Two distinct defects in intracellular growth complemented by a single genetic locus in *Legionella pneumophila*. *Mol Microbiol* **7**, 7-19 (1993).

12. Burstein, D. *et al.* Genomic analysis of 38 *Legionella* species identifies large and diverse effector repertoires. *Nat Genet* **48**, 167-175 (2016).

13. Gomez-Valero, L. *et al.* More than 18,000 effectors in the *Legionella* genus genome provide multiple, independent combinations for replication in human cells. *Proc Natl Acad Sci U S A* **116**, 2265-2273 (2019).

14. Qiu, J. & Luo, Z.Q. *Legionella* and *Coxiella* effectors: strength in diversity and activity. *Nat Rev Microbiol* **15**, 591-605 (2017).

15. Creasey, E.A. & Isberg, R.R. The protein SdhA maintains the integrity of the *Legionella*-containing vacuole. *Proc Natl Acad Sci U S A* **109**, 3481-3486 (2012).

16. Steiner, B., Weber, S. & Hilbi, H. Formation of the *Legionella*-containing vacuole: phosphoinositide conversion, GTPase modulation and ER dynamics. *Int J Med Microbiol* **308**, 49-57 (2018).

17. Gaspar, A.H. & Machner, M.P. VipD is a Rab5-activated phospholipase A1 that protects *Legionella pneumophila* from endosomal fusion. *Proc Natl Acad Sci U S A* **111**, 4560-4565 (2014).

18. Belyi, Y. *et al. Legionella pneumophila* glucosyltransferase inhibits host elongation factor 1A. *Proc Natl Acad Sci U S A* **103**, 16953-16958 (2006).

19. Jeong, K.C., Sexton, J.A. & Vogel, J.P. Spatiotemporal regulation of a *Legionella pneumophila* T4SS substrate by the metaeffector SidJ. *PLoS Pathog* **11**, e1004695 (2015).

20. Qiu, J. *et al.* Ubiquitination independent of E1 and E2 enzymes by bacterial effectors. *Nature* **533**, 120-124 (2016).

21. Bhogaraju, S. *et al.* Phosphoribosylation of Ubiquitin Promotes Serine Ubiquitination and Impairs Conventional Ubiquitination. *Cell* **167**, 1636-1649 e1613 (2016).

22. Kotewicz, K.M. *et al.* A Single *Legionella* Effector Catalyzes a Multistep Ubiquitination Pathway to Rearrange Tubular Endoplasmic Reticulum for Replication. *Cell Host Microbe* **21**, 169-181 (2017).

23. Song, L. *et al.* The *Legionella* Effector SdjA Is a Bifunctional Enzyme That Distinctly Regulates Phosphoribosyl Ubiquitination. *mBio* **12**, e0231621 (2021).

24. Sulpizio, A. *et al.* Protein polyglutamylation catalyzed by the bacterial calmodulin-dependent pseudokinase SidJ. *Elife* **8** (2019).

25. Bhogaraju, S. *et al.* Inhibition of bacterial ubiquitin ligases by SidJ-calmodulin catalysed glutamylation. *Nature* **572**, 382-386 (2019).

26. Black, M.H. *et al.* Bacterial pseudokinase catalyzes protein polyglutamylation to inhibit the SidE-family ubiquitin ligases. *Science* **364**, 787-792 (2019).

27. Wan, M. *et al.* Deubiquitination of phosphoribosyl-ubiquitin conjugates by phosphodiesterase-domain-containing *Legionella* effectors. *Proc Natl Acad Sci U S A* **116**, 23518-23526 (2019).

28. Shin, D. *et al.* Regulation of Phosphoribosyl-Linked Serine Ubiquitination by Deubiquitinases DupA and DupB. *Mol Cell* **77**, 164-179 e166 (2020).

29. Akturk, A. *et al.* Mechanism of phosphoribosyl-ubiquitination mediated by a single *Legionella* effector. *Nature* **557**, 729-733 (2018).

30. Kalayil, S. *et al.* Insights into catalysis and function of phosphoribosyl-linked serine ubiquitination. *Nature* **557**, 734-738 (2018).

31. Dong, Y. *et al.* Structural basis of ubiquitin modification by the *Legionella* effector SdeA. *Nature* **557**, 674-678 (2018).

32. Sheedlo, M.J. *et al.* Structural basis of substrate recognition by a bacterial deubiquitinase important for dynamics of phagosome ubiquitination. *Proc Natl Acad Sci U S A* **112**, 15090-15095 (2015).

33. Zhang, M. *et al.* Members of the *Legionella pneumophila* Sde family target tyrosine residues for phosphoribosyl-linked ubiquitination. *RSC Chem Biol* **2**, 1509-1519 (2021).

34. Liu, Y. *et al.* Serine-ubiquitination regulates Golgi morphology and the secretory pathway upon *Legionella* infection. *Cell Death Differ* **28**, 2957-2969 (2021).

35. Kim, S. & Isberg, R.R. The Sde phosphoribosyl-linked ubiquitin transferases protect the *Legionella pneumophila* vacuole from degradation by the host. *Proc Natl Acad Sci U S A* **120**, e2303942120 (2023).

36. Bruckert, W.M. & Abu Kwaik, Y. Lysine11-Linked Polyubiquitination of the AnkB F-Box Effector of *Legionella pneumophila*. *Infect Immun* **84**, 99-107 (2016).

37. Ivanov, S.S. & Roy, C.R. Modulation of ubiquitin dynamics and suppression of DALIS formation by the *Legionella pneumophila* Dot/Icm system. *Cell Microbiol* **11**, 261-278 (2009).

38. Horenkamp, F.A. *et al. Legionella pneumophila* subversion of host vesicular transport by SidC effector proteins. *Traffic* **15**, 488-499 (2014).

39. Hsu, F. *et al.* The *Legionella* effector SidC defines a unique family of ubiquitin ligases important for bacterial phagosomal remodeling. *Proc Natl Acad Sci U S A* **111**, 10538-10543 (2014).

40. Dorer, M.S., Kirton, D., Bader, J.S. & Isberg, R.R. RNA interference analysis of *Legionella* in Drosophila cells: exploitation of early secretory apparatus dynamics. *PLoS Pathog* **2**, e34 (2006).

41. Tomaskovic, I., Gonzalez, A. & Dikic, I. Ubiquitin and *Legionella*: From bench to bedside. *Semin Cell Dev Biol* (2022).

42. Puvar, K. *et al.* Ubiquitin Chains Modified by the Bacterial Ligase SdeA Are Protected from Deubiquitinase Hydrolysis. *Biochemistry* **56**, 4762-4766 (2017).

43. Boyle, K.B. & Randow, F. The role of 'eat-me' signals and autophagy cargo receptors in innate immunity. *Curr Opin Microbiol* **16**, 339-348 (2013).

44. von Muhlinen, N. *et al.* An essential role for the ATG8 ortholog LC3C in antibacterial autophagy. *Autophagy* **9**, 784-786 (2013).

45. Mitchell, G. & Isberg, R.R. Innate Immunity to Intracellular Pathogens: Balancing Microbial Elimination and Inflammation. *Cell Host Microbe* **22**, 166-175 (2017).

46. Choy, A. *et al.* The *Legionella* effector RavZ inhibits host autophagy through irreversible Atg8 deconjugation. *Science* **338**, 1072-1076 (2012).

47. Arasaki, K. & Tagaya, M. *Legionella* blocks autophagy by cleaving STX17 (syntaxin 17). *Autophagy* **13**, 2008-2009 (2017).

48. Omotade, T.O. & Roy, C.R. *Legionella pneumophila* Excludes Autophagy Adaptors from the Ubiquitin-Labeled Vacuole in Which It Resides. *Infect Immun* **88** (2020).

49. Wan,M., *et al*. Phosphoribosyl modification of poly-ubiquitin chains at the *Legionella*-containing vacuole prohibiting autophagy adaptor recognition. *Submitted* (2023).

50. Isogai, S. *et al.* Crystal structure of the ubiquitin-associated (UBA) domain of p62 and its interaction with ubiquitin. *J Biol Chem* **286**, 31864-31874 (2011).

51. Johansen, T. & Lamark, T. Selective autophagy mediated by autophagic adapter proteins. *Autophagy* **7**, 279-296 (2011).

52. Long, J. *et al.* Ubiquitin recognition by the ubiquitin-associated domain of p62 involves a novel conformational switch. *J Biol Chem* **283**, 5427-5440 (2008).

53. Long, J. *et al.* Dimerisation of the UBA domain of p62 inhibits ubiquitin binding and regulates NF-kappaB signalling. *J Mol Biol* **396**, 178-194 (2010).

54. Tan, X.L. *et al.* Sortase-mediated chemical protein synthesis reveals the bidentate binding of bisphosphorylated p62 with K63 diubiquitin. *Chem Sci* **8**, 6881-6887 (2017).

55. Gan, N. *et al.* Regulation of phosphoribosyl ubiquitination by a calmodulin-dependent glutamylase. *Nature* **572**, 387-391 (2019).

56. Ge, J. *et al.* Phosphoribosyl-linked serine ubiquitination of USP14 by the SidE family effectors of *Legionella* excludes p62 from the bacterial phagosome. *Cell Rep* **42**, 112817 (2023).

57. Bhogaraju, S. & Dikic, I. Cell biology: Ubiquitination without E1 and E2 enzymes. *Nature* **533**, 43-44 (2016).

58. Kozlov, G. *et al.* Structural basis of ubiquitin recognition by the ubiquitin-associated (UBA) domain of the ubiquitin ligase EDD. *J Biol Chem* **282**, 35787-35795 (2007).

59. Ensminger, A.W. & Isberg, R.R. E3 ubiquitin ligase activity and targeting of BAT3 by multiple *Legionella pneumophila* translocated substrates. *Infect Immun* **78**, 3905-3919 (2010).

60. Hubber, A., Kubori, T. & Nagai, H. Modulation of the ubiquitination machinery by *Legionella*. *Curr Top Microbiol Immunol* **376**, 227-247 (2013).

61. Nagai, H. & Kubori, T. Purification and characterization of *Legionella* U-box-type E3 ubiquitin ligase. *Methods Mol Biol* **954**, 347-354 (2013).

62. Liu, S. *et al.* Interplay between bacterial deubiquitinase and ubiquitin E3 ligase regulates ubiquitin dynamics on *Legionella* phagosomes. *Elife* **9** (2020).

63. Ong, S.Y. *et al.* Genome-wide genetic screen identifies host ubiquitination as important for *Legionella pneumophila* Dot/Icm effector translocation. *Cell Microbiol* **23**, e13368 (2021).

64. Goodall, E.A., Kraus, F. & Harper, J.W. Mechanisms underlying ubiquitin-driven selective mitochondrial and bacterial autophagy. *Mol Cell* **82**, 1501-1513 (2022).

65. Sharma, V., Verma, S., Seranova, E., Sarkar, S. & Kumar, D. Selective Autophagy and Xenophagy in Infection and Disease. *Front Cell Dev Biol* **6**, 147 (2018).

66. Faucher, S.P., Mueller, C.A. & Shuman, H.A. *Legionella pneumophila* Transcriptome during Intracellular Multiplication in Human Macrophages. *Front Microbiol* **2**, 60 (2011).

67. Jeong, K.C., Sutherland, M.C. & Vogel, J.P. Novel export control of a *Legionella* Dot/Icm substrate is mediated by dual, independent signal sequences. *Mol Microbiol* **96**, 175-188 (2015).

68. Bardill, J.P., Miller, J.L. & Vogel, J.P. IcmS-dependent translocation of SdeA into macrophages by the *Legionella pneumophila* type IV secretion system. *Mol Microbiol* **56**, 90-103 (2005).

69. O'Connor, T.J., Boyd, D., Dorer, M.S. & Isberg, R.R. Aggravating genetic interactions allow a solution to redundancy in a bacterial pathogen. *Science* **338**, 1440-1444 (2012).

70. Berger, K.H., Merriam, J.J. & Isberg, R.R. Altered intracellular targeting properties associated with mutations in the *Legionella pneumophila* dotA gene. *Mol Microbiol* **14**, 809-822 (1994).

71. Byrne, B. & Swanson, M.S. Expression of *Legionella pneumophila* virulence traits in response to growth conditions. *Infect Immun* **66**, 3029-3034 (1998).

72. Haenssler, E., Ramabhadran, V., Murphy, C.S., Heidtman, M.I. & Isberg, R.R. Endoplasmic Reticulum Tubule Protein Reticulon 4 Associates with the *Legionella pneumophila* Vacuole and with Translocated Substrate Ceg9. *Infect Immun* **83**, 3479-3489 (2015).

73. Treier, M., Staszewski, L.M. & Bohmann, D. Ubiquitin-dependent c-Jun degradation in vivo is mediated by the delta domain. *Cell* **78**, 787-798 (1994).

74. Derre, I. & Isberg, R.R. LidA, a translocated substrate of the *Legionella pneumophila* type IV secretion system, interferes with the early secretory pathway. *Infect Immun* **73**, 4370-4380 (2005).

75. Schindelin, J. *et al.* Fiji: an open-source platform for biological-image analysis. *Nat Methods* **9**, 676-682 (2012).

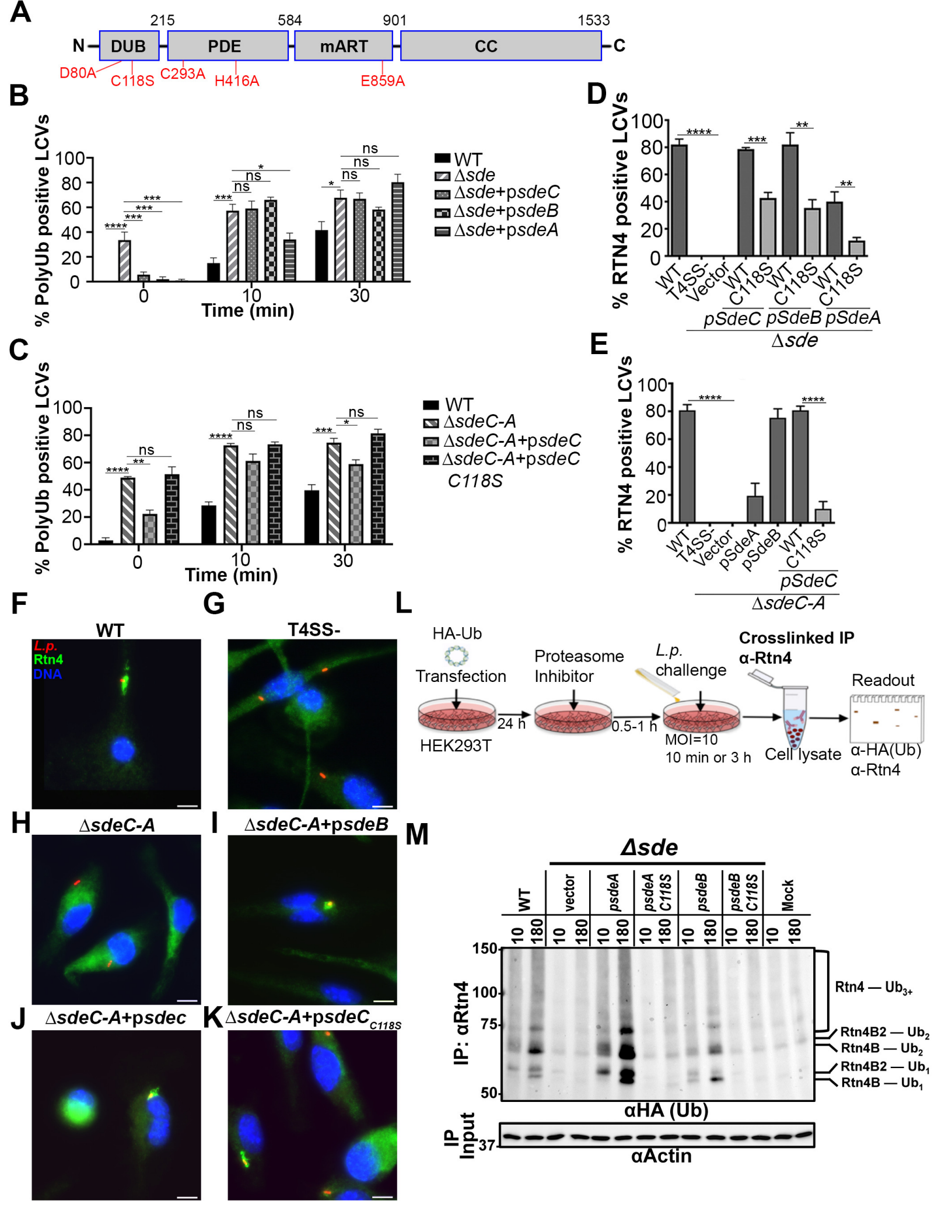
A
215
584
901
1533
N
DUB
PDE
mART
CC
C
D80A
C118S
C293A
H416A
E859A
B
% PolyUb positive LCVs
Time (min)
WT
Δsde
Δsde+psdeC
Δsde+psdeB
Δsde+psdeA
C
ΔsdeC-A
ΔsdeC-A+psdeC
ΔsdeC-A+psdeC C118S
D
% RTN4 positive LCVs
WT
T4SS-
Vector
C118S
pSdeC
pSdeB
pSdeA
Δsde
E
pSdeA
pSdeB
ΔsdeC-A
F
G
WT
T4SS-
L.p.
Rtn4
DNA
H
ΔsdeC-A
I
ΔsdeC-A+psdeB
J
ΔsdeC-A+psdec
K
ΔsdeC-A+psdeC C118S
L
HA-Ub
Transfection
HEK293T
24 h
Proteasome Inhibitor
0.5-1 h
L.p. challenge
MOI=10
10 min or 3 h
Crosslinked IP α-Rtn4
Cell lysate
Readout
α-HA(Ub)
α-Rtn4
M
Δsde
WT
vector
psdeA
psdeA C118S
psdeB
psdeB C118S
Mock
IP: αRtn4
Rtn4 — Ub3+
Rtn4B2 — Ub2
Rtn4B — Ub2
Rtn4B2 — Ub1
Rtn4B — Ub1
αHA (Ub)
IP
Input
αActin

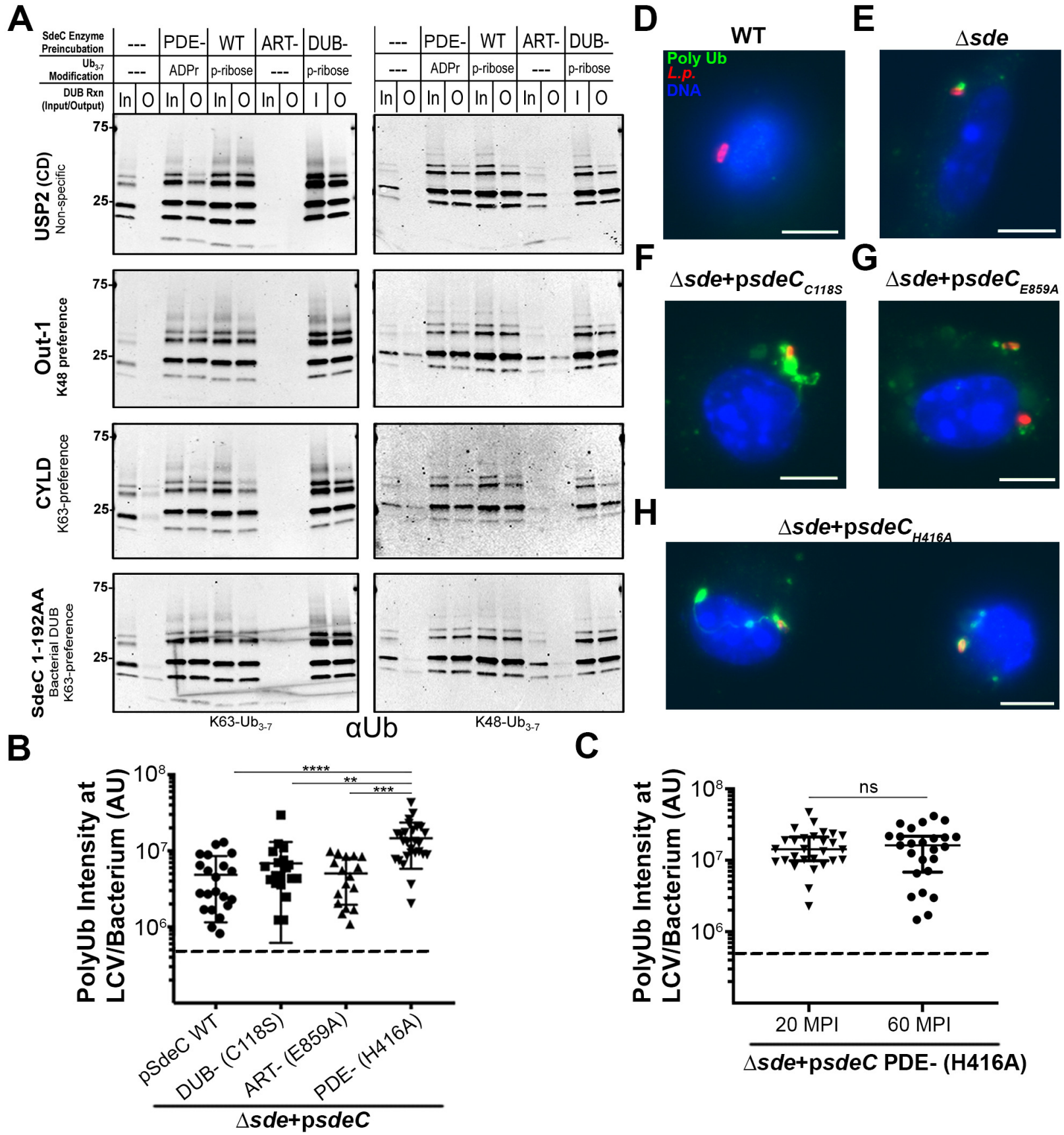
A
SdeC Enzyme Preincubation

PDE-
WT
ART-
DUB-
Ub3-7 Modification
ADPr
p-ribose
DUB Rxn (Input/Output)
In
O
I
USP2 (CD)
Non-specific
Out-1
K48 preference
CYLD
K63-preference
SdeC 1-192AA
Bacterial DUB
K63-preference
75
25
K63-Ub3-7
αUb
K48-Ub3-7
B
PolyUb Intensity at LCV/Bacterium (AU)
10^8
10^7
10^6
****
**
***
pSdeC WT
DUB- (C118S)
ART- (E859A)
PDE- (H416A)
Δsde+psdeC
C
ns
20 MPI
60 MPI
Δsde+psdeC PDE- (H416A)
D
WT
Poly Ub
L.p.
DNA
E
Δsde
F
Δsde+psdeC C118S
G
Δsde+psdeC E859A
H
Δsde+psdeC H416A

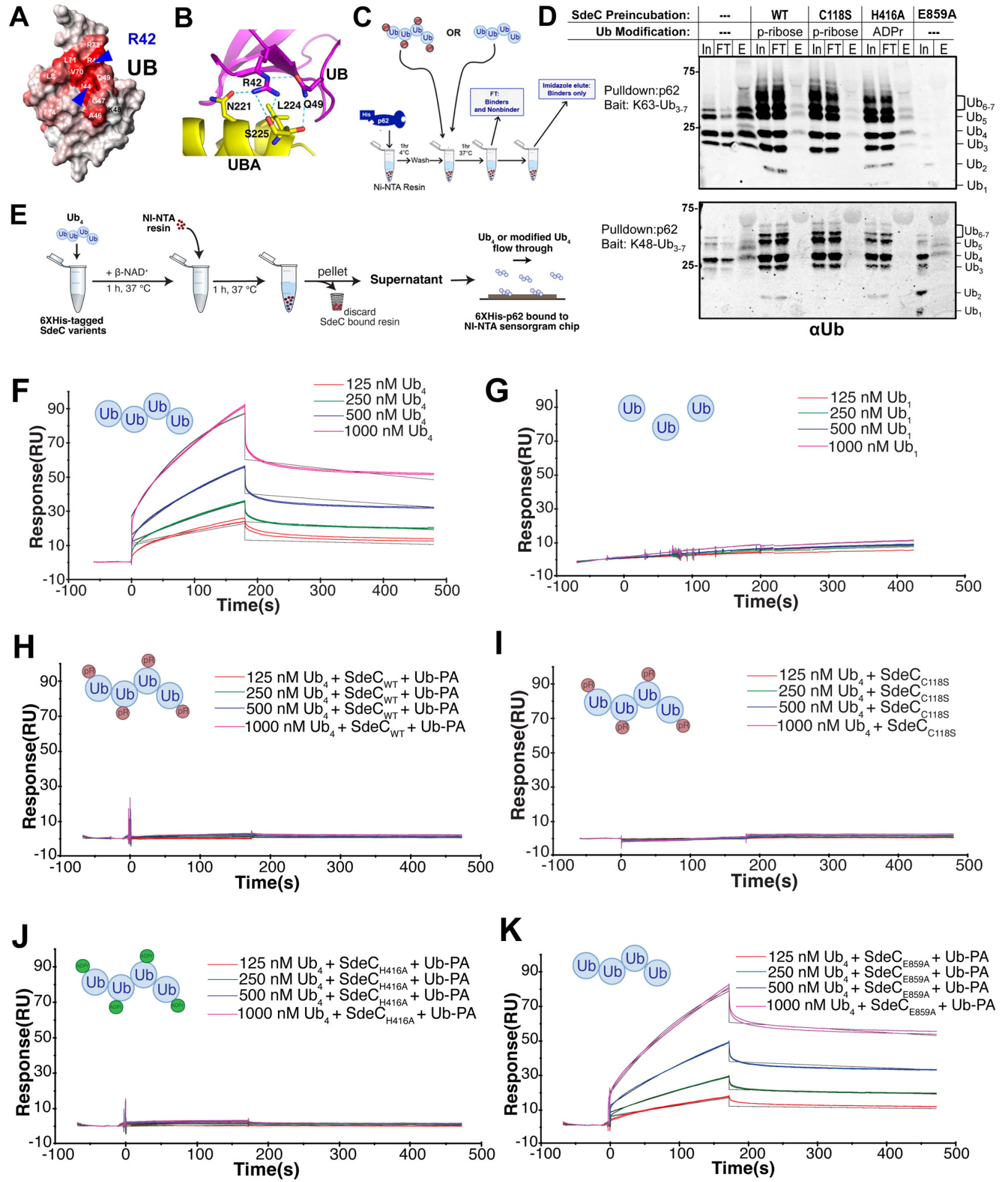
A
R42
UB
B
R42
UB
N221
L224
Q49
S225
UBA
C
OR
His
p62
1hr 4°C
Wash
1hr 37°C
FT: Binders and Nonbinder
Imidazole elute: Binders only
Ni-NTA Resin
D
SdeC Preincubation: --- WT C118S H416A E859A
Ub Modification: --- p-ribose p-ribose ADPr ---
In FT E In FT E In FT E In FT E In E
Pulldown:p62
Bait: K63-Ub3-7
Pulldown:p62
Bait: K48-Ub3-7
Ub6-7
Ub5
Ub4
Ub3
Ub2
Ub1
αUb
E
Ub4
NI-NTA resin
+ β-NAD+
1 h, 37 °C
1 h, 37 °C
pellet
Supernatant
discard SdeC bound resin
Ub4 or modified Ub4 flow through
6XHis-tagged SdeC varients
6XHis-p62 bound to NI-NTA sensorgram chip
F
125 nM Ub4
250 nM Ub4
500 nM Ub4
1000 nM Ub4
Response(RU)
Time(s)
G
125 nM Ub1
250 nM Ub1
500 nM Ub1
1000 nM Ub1
Response(RU)
Time(s)
H
125 nM Ub4 + SdeCWT + Ub-PA
250 nM Ub4 + SdeCWT + Ub-PA
500 nM Ub4 + SdeCWT + Ub-PA
1000 nM Ub4 + SdeCWT + Ub-PA
Response(RU)
Time(s)
I
125 nM Ub4 + SdeCC118S
250 nM Ub4 + SdeCC118S
500 nM Ub4 + SdeCC118S
1000 nM Ub4 + SdeCC118S
Response(RU)
Time(s)
J
125 nM Ub4 + SdeCH416A + Ub-PA
250 nM Ub4 + SdeCH416A + Ub-PA
500 nM Ub4 + SdeCH416A + Ub-PA
1000 nM Ub4 + SdeCH416A + Ub-PA
Response(RU)
Time(s)
K
125 nM Ub4 + SdeCE859A + Ub-PA
250 nM Ub4 + SdeCE859A + Ub-PA
500 nM Ub4 + SdeCE859A + Ub-PA
1000 nM Ub4 + SdeCE859A + Ub-PA
Response(RU)
Time(s)

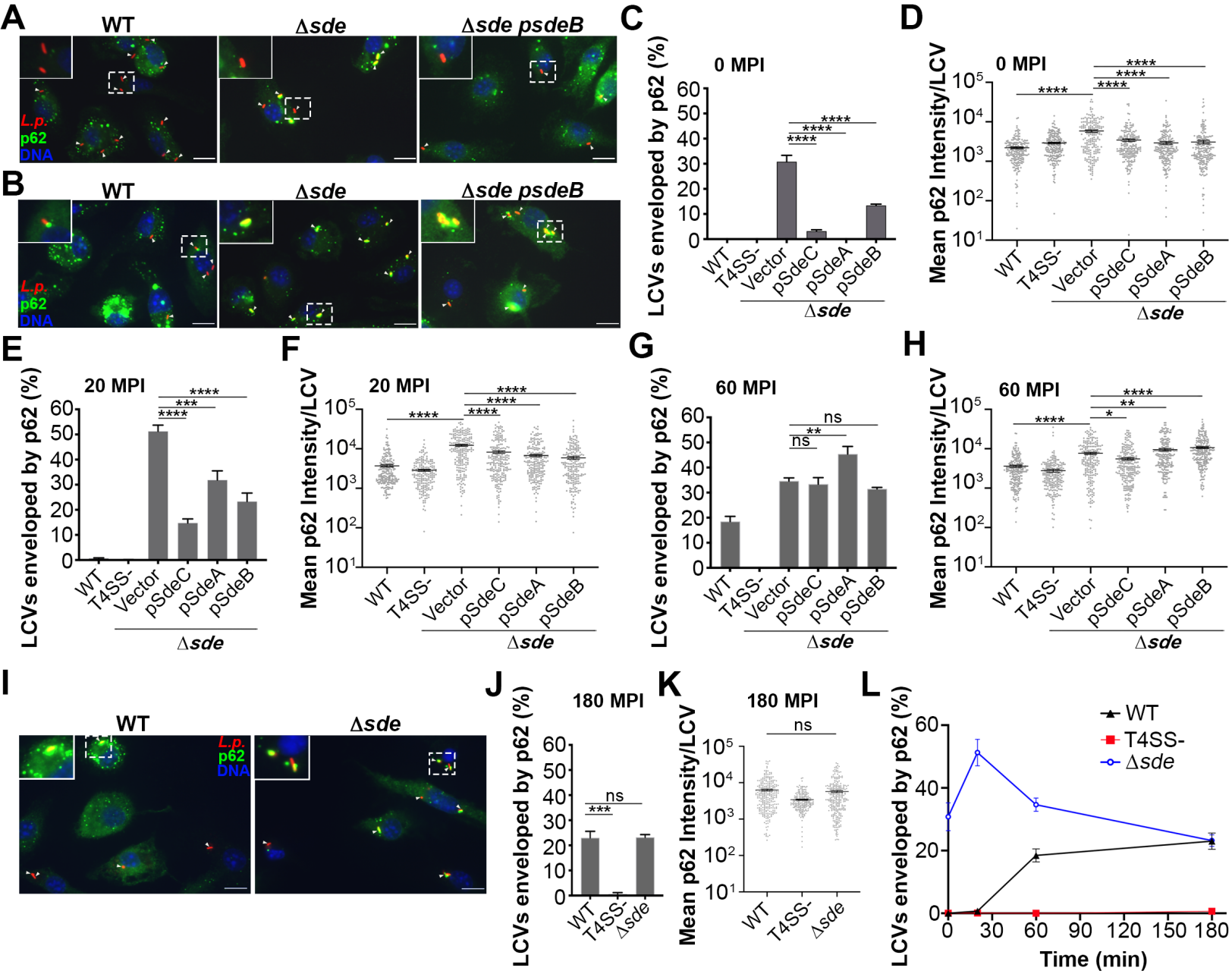
A
WT
Δsde
Δsde psdeB
L.p.
p62
DNA
B
C
0 MPI
LCVs enveloped by p62 (%)
WT
T4SS-
Vector
pSdeC
pSdeA
pSdeB
Δsde
D
Mean p62 Intensity/LCV
E
20 MPI
F
G
60 MPI
H
I
J
180 MPI
K
L
WT
T4SS-
Δsde
Time (min)
ns

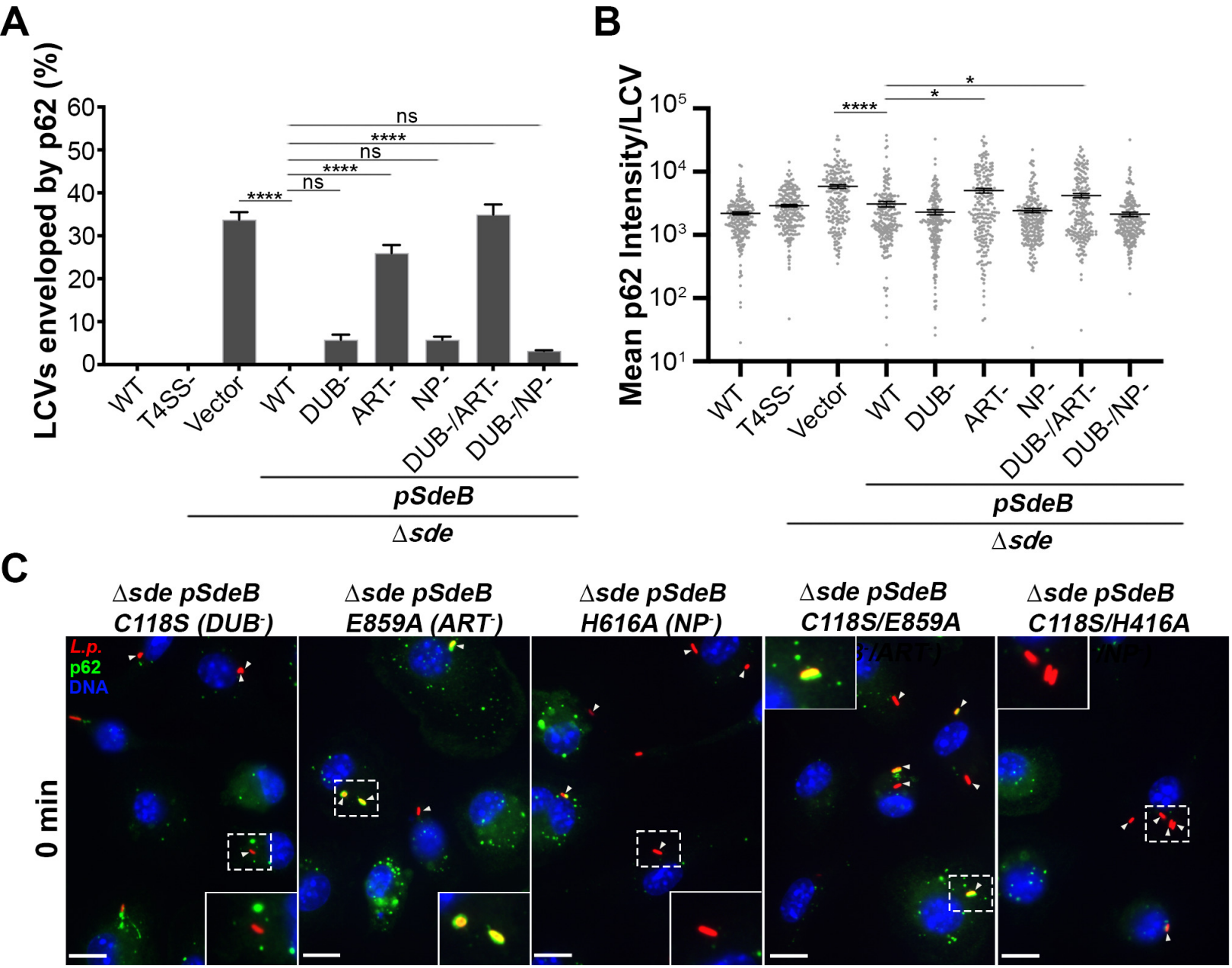
A
LCVs enveloped by p62 (%)
60
50
40
30
20
10
0
ns
****
ns
****
ns
****
WT
T4SS-
Vector
WT
DUB-
ART-
NP-
DUB-/ART-
DUB-/NP-
pSdeB
Δsde
B
Mean p62 Intensity/LCV
10^5
10^4
10^3
10^2
10^1
*
*
****
WT
T4SS-
Vector
WT
DUB-
ART-
NP-
DUB-/ART-
DUB-/NP-
pSdeB
Δsde
C
Δsde pSdeB C118S (DUB-)
Δsde pSdeB E859A (ART-)
Δsde pSdeB H616A (NP-)
Δsde pSdeB C118S/E859A
Δsde pSdeB C118S/H416A
L.p.
p62
DNA
0 min

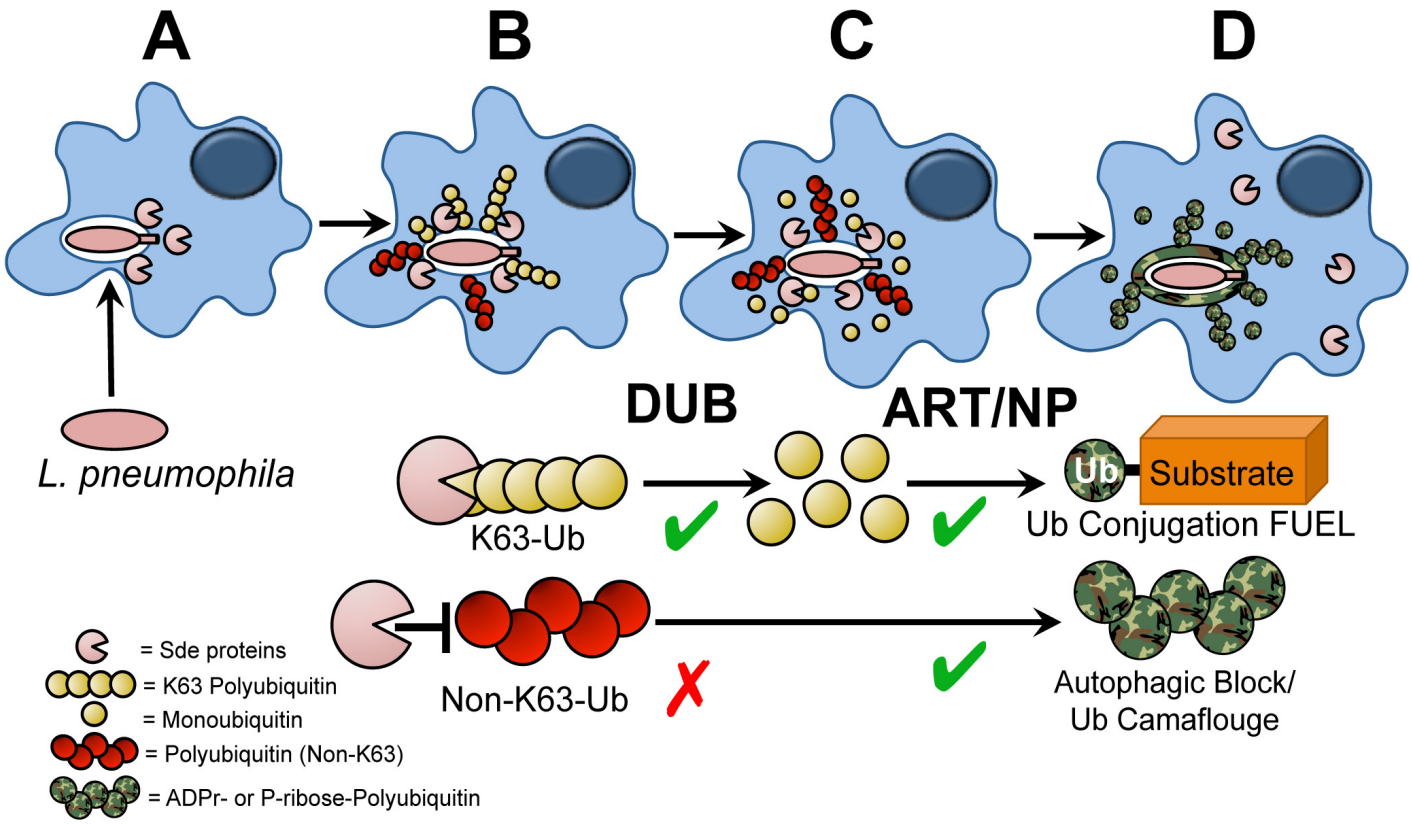
A
B
C
D
L. pneumophila
DUB
ART/NP
K63-Ub
Ub
Substrate
Ub Conjugation FUEL
Non-K63-Ub
Autophagic Block/
Ub Camaflouge
= Sde proteins
= K63 Polyubiquitin
= Monoubiquitin
= Polyubiquitin (Non-K63)
= ADPr- or P-ribose-Polyubiquitin